

Enhancement of Thermal Contact Conductance of Coated Junctions

Kee-Chiang Chung*

National Yunlin Institute of Technology, Yunlin 640, Taiwan, Republic of China
and

John W. Sheffield†

University of Missouri–Rolla, Rolla, Missouri 65401

The thermal contact conductance of coated, contacting aluminum 6061-T651 surfaces was studied experimentally. Four different coating materials, copper, silver, a phase mixture of copper-carbon, and a phase mixture of silver-carbon were evaluated using four different surface roughnesses for each coating material. All of the samples were tested at contact pressures of 125, 250, 375, and 500 kPa. The test results of thermal contact conductance are presented in terms of coating thickness, surface texture, and properties of the coating materials. Using the experimental data, dimensionless expressions were developed that relate the contact conductance of the phase mixture and pure coatings to the coating thickness, the surface roughness, the contact pressure, and the properties of the aluminum substrate. The effects of the surface roughness and of the phase mixture of the coatings on the thermal contact conductance were investigated. In addition, the load cycling effect on the thermal contact conductance was examined for bare aluminum 6061-T651 specimens.

Nomenclature

- c_1 = Vickers microhardness coefficient
- c_2 = Vickers microhardness coefficient
- e = surface asperity slope
- H = microhardness of uncoated specimens, Pa
- H' = microhardness of coated specimens, Pa
- H_m = hardness of the surface of a layer, Pa
- h = thermal contact conductance without a coating layer, $\text{W/m}^2\text{K}$
- h' = thermal contact conductance with a coating layer, $\text{W/m}^2\text{K}$
- h_c = overall contact conductance, $\text{W/m}^2\text{K}$
- k = thermal conductivity, W/mK
- k' = harmonic mean thermal conductivity, W/mK
- P = contact pressure, Pa
- Ra = arithmetic average roughness, μm
- T = temperature, K
- t = coating layer thickness, μm
- β = coefficient of linear expression
- σ = surface roughness, μm

Introduction

IN recent years there have been significant advances in theoretical and experimental correlation models used to predict the thermal contact conductance across bare junctions. Models and correlations suitable for selected conditions and geometries have been developed. The current theories can predict, with moderate accuracy, the temperature drop across a metal interface or the thermal contact conductance of flat, rough contacting uncoated metallic surfaces, provided that basic thermophysical properties are known.¹

When two surfaces are brought into contact, a relatively high thermal resistance occurs because an imperfect junction exists. Several interstitial techniques can enhance the heat

transfer across the bare joint, such as the application of a thermal grease to the contacting surfaces, insertion of a soft metal foil in the interface, or coating one or both of the contacting surfaces. Clearly, these enhancement techniques will be relative, in part, to bare contacts. Numerous investigations have focused on the enhancement of thermal contact conductance using interstitial techniques.² Thermal grease application may be the most desirable of these three techniques for general applications. However, there is the possibility of contaminating other sensitive components nearby. Metal foils should be very soft and very thin. Conceptually, soft metallic coatings have several desirable characteristics, such as ease of handling. Hence, the use of metallic coatings appears to be suitable as a candidate for applications such as electronic and spacecraft system thermal control because of the limitations of contamination by greases and handling difficulties of the thin foils.

In the past decade, as the size of electronic components has decreased, greater importance has been placed on the application of advanced thermal control techniques. The improvements in microelectronics and ultra large scale integration (ULSI) techniques caused the number of devices at the chip level to increase from 10 to 100,000 devices/chip. The circuit power has also grown to accommodate faster circuit speeds.³ Hence, the heat flux levels within these devices have increased by several orders of magnitude. The heat generation within the high density devices such as multichip modules, multilayer printed-circuit boards, and integrated circuit chips, will cause thermal failure⁴ if some appropriate techniques to solve these problems are not found. Therefore, design consideration to reduce the interface resistance is highly desirable since this resistance results in increased operation temperatures. In an effort to find the thermal contact resistance of the bonding materials in the bonded joint for silicon chips, Peterson and Fletcher⁵ conducted an experiment that evaluated seven conducting epoxies with thermal conductivities ranging from 0.27 to 1.93 W/mC , in contact with ground aluminum 6060-T6 surfaces. An expression for predicting the overall joint resistance was developed. Eid and Antonetti⁶ designed a small-scale experiment to measure the thermal contact resistance of aluminum in contact with silicon. A 2×2 -mm aluminum test section was made and the contact

Received Nov. 1, 1993; revision received Sept. 26, 1994; accepted for publication Sept. 27, 1994. Copyright © 1994 by the American Institute of Aeronautics and Astronautics, Inc. All rights reserved.

*Associate Professor, Department of Mechanical Engineering.

†Professor, Department of Mechanical and Aerospace Engineering. Senior Member AIAA.

pressure was varied from 27 to 500 kPa. The results showed agreement with correlations developed by Yovanovich.⁷

One of the effective techniques to improve the thermal performance and reliability of microelectronic systems is to enhance the heat transfer at interfaces between the substrate and mold compound materials. Several techniques of thermal enhancement for electronic systems are suitable for increasing the thermal contact conductance of microelectronic components. Fletcher⁸ divided these techniques into four major categories: 1) grease and oils, 2) metallic foils and screens, 3) composite materials, and 4) surface treatments (coatings). These techniques have distinct physical and chemical composition.

For a coated joint, a model using an effective hardness and effective thermal conductivity was proposed by Antonetti and Yovanovich.⁹ The model for the thermal contact conductance of the joint with two coated surfaces was given as

$$h' = h(H/H')^{0.93}[(k_1 + k_2)/(k_2 C_1 + k_1 C_2)] \quad (1)$$

The results from this model were shown to compare quite well with their experimental data. Two-surface coatings were compared to one-surface coatings by Chung et al.¹⁰ for aluminum, lead, and indium coating materials. The thermal contact conductance was found to vary from 0 to 500% of the uncoated value, depending on the contact surface characteristics. Fletcher et al.¹¹ developed a dimensionless correlation for the thermal contact conductance of multilayered metallic sheets. The experimental data were obtained using aluminum samples whose thicknesses ranged from 0.035 to 0.3074 cm for contact pressures of 0.689–10.34 MPa. The resulting expressions were presented as a function of dimensionless parameters for the layer material, apparent contact pressure, and mean junction temperature. The correlation is

$$(h_c t/k) = 40,000(\beta T)(P/H_m)^{1.15} \quad (2)$$

for thick gauge samples (2.896–3.056 mm thickness) and

$$(h_c t/k) = 2,500(\beta T)(P/H_m)^{0.97} \quad (3)$$

for thin gauge samples (0.305–0.457 mm thickness).

Kang et al.¹² conducted an experiment to investigate the coating effect on the thermal contact conductance for turned surfaces. Three different materials, lead, tin, and indium, were evaluated using four different coating thicknesses, and the results verified that an optimum coating thickness existed. However, the effect of surface roughness on the enhancement of the thermal contact conductance was not examined.

Thermal Contact Conductance Evaluation

In order to determine the thermal contact conductance of the phase mixture copper-carbon/silver-carbon and pure copper/silver coatings, an experimental investigation was conducted. Specimens were tested with four different surface roughnesses, polished, turned, blasted-smooth, and blasted-rough, with 0.19 to 0.45 μm coating thickness. Profilometer measurements of the contacting surfaces indicated the average surface roughness ranged from 0.18 to 7.92 μm using a Perthometer model C5D made by Feinprueft Corporation. Pertinent test specimen characteristics are shown in Table 1.

Experimental Facility

A series of static tests have been made to determine the effects of surface characteristics and contact pressures on various coating materials. A schematic of the test setup is shown in Fig. 1. Two samples, with their coated surfaces facing together, are placed in vertical alignment with the two heat flow meters. Each heat flow meter, which is made of 304 stainless steel, is approximately 10.16 cm long and 2.54 cm in diam. Four 1.27-cm-deep and 1.59-mm-diam holes were drilled perpendicular to the axes of each heat flow meter to accom-

Table 1 Surface characteristics of test specimens

Finished type	Pair no.	e , rad	Ra , μm	Coating materials	t , μm
Polished	1	0.032	0.23	Cu-C	0.25
	5	0.018	0.18	None	None
	9	0.038	0.29	Cu	0.19
	13	0.034	0.25	Ag	0.23
	17	0.045	0.31	Ag-C	0.18
Turned	2	0.066	0.39	Cu-C	0.45
	6	0.045	0.40	None	None
	10	0.069	0.43	Cu	0.19
	14	0.088	0.45	Ag	0.23
	18	0.045	0.35	Ag-C	0.18
Blasted smooth	3	0.34	2.53	Cu-C	0.45
	7	0.23	4.53	None	None
	11	0.39	4.25	Cu	0.24
	15	0.35	3.16	Ag	0.24
	19	0.41	2.89	Ag-C	0.39
Blasted rough	4	0.55	5.02	Cu-C	0.25
	8	0.28	7.92	None	None
	12	0.43	5.03	Cu	0.24
	16	0.48	4.38	Ag	0.24
	20	0.59	4.43	Ag-C	0.39

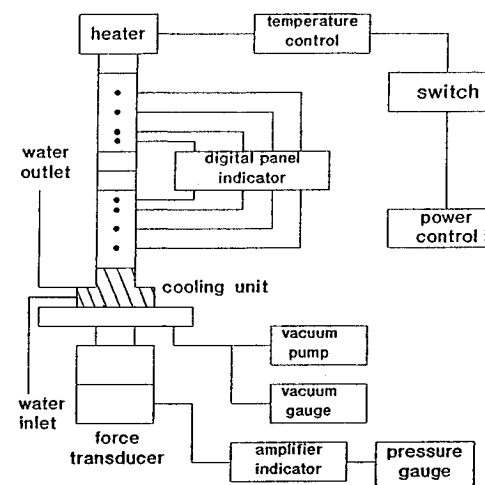


Fig. 1 Schematic diagram of measurement and control system.

modate thermocouples. Upon installation of these thermocouples, a thermal grease was used to fill these holes. Figure 2 shows the exact flow meter dimensions and the locations of the thermocouple holes, as well as the heat flow meter positions relative to the test samples. The combination of the heat flow meters and the samples may be referred to as the "test stack."

A heating and cooling system was employed to create a one-dimensional, steady heat flow across the test interface in this thermal test. The heat flow was supplied to the top of the test stack, with an electrical resistance heater. Axial heat loss out the top was controlled by inserting an insulating spacer between the heater and the upper support plate. The temperature at the interface was maintained constant using a thermocouple controller. The cooling system was placed at the bottom of the test stack. An open-loop cooling water system was used. Contact pressures were applied with a push-rod attached to a pneumatic pressure cylinder that activated a bellows. The entire vertical system, which includes the heater, heat flow meters, test samples, and heat sink was placed on this bellows. The force present in the stack was measured with a calibrated device consisting of a load cell, transducer, air cylinder, and the base plate. This air cylinder was activated gradually to avoid impact forces that might damage the coating layer. The heater, cooler, heat flow meters and samples were checked for alignment. All tests were conducted in a vacuum created by a vacuum pump and bell jar arrangement

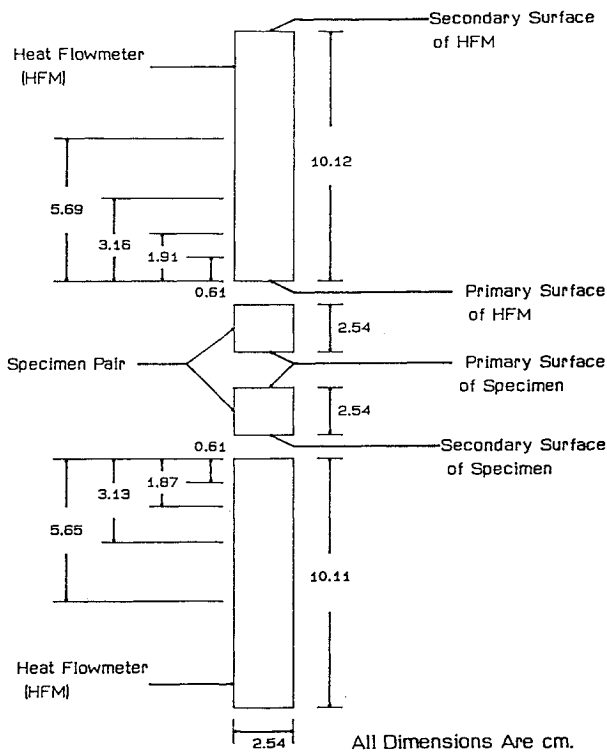


Fig. 2 Schematic of test column.

capable of reaching 0.2 T, which is well below the minimum required vacuum of 1 mm Hg for eliminating convective heat transfer.¹³

Experimental Procedure

The initial experimental tests were conducted to examine the thermal contact conductance of test specimens with coatings compared with those without coatings. The uncoated samples were tested first to establish a baseline of thermal contact conductance values for each coating pair. The experimental procedure for all of the thermal tests was as follows: using acetone and a lint free cloth. Clean each secondary surface of the specimen and the primary surface of both heat flow meters. Carefully place the specimen pair between the heat flow meters and test alignment of the vertical stack. Reseat the bell jar on the vacuum base. Approximately 6 h were needed to outgas the specimens and to achieve a stable vacuum level. Test runs were performed at an average interface temperature of $60 \pm 2^\circ\text{C}$. The heat flux through the interface was considered to be the mean of the thermal fluxes through the heat flow meters. The heat flux of upper heat flux meter was typically estimated 18% higher than the lower heat flux meter. The thermal contact conductance was then computed from the average heat flux divided by the temperature drop at the interface. To determine the temperature drop at the interface, the upper and lower temperature gradients were extrapolated to the upper and lower primary surfaces of the specimens, respectively. For each test specimen pair, the contact loading pressure was increased from approximately 125 to 500 kPa, and back to 125 in 125 kPa increments.

An experimental investigation is not complete without estimation of the uncertainties associated with the measured values. Using the uncertainty resulting from the thermocouple accuracy and extrapolation of the temperature gradients, the overall experimental uncertainty was estimated to be $\pm 8\%$.

Results and Discussion

The results of the experimental test program for uncoated samples are presented graphically in Fig. 3, showing the ther-

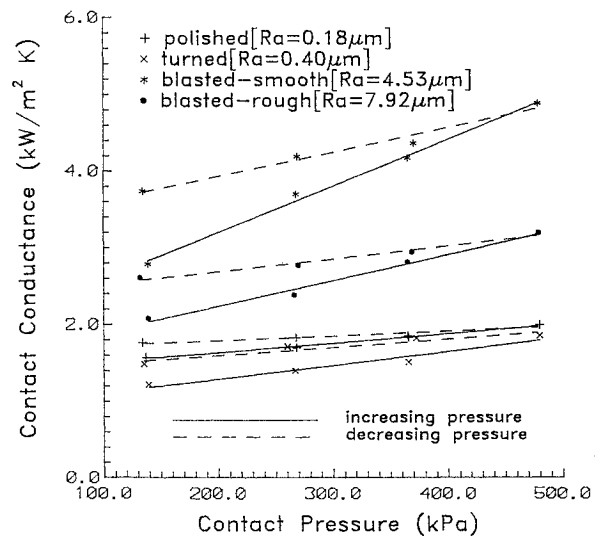


Fig. 3 Uncoated test results.

mal contact conductance as a function of the contact pressure. Another important phenomenon of contact conductance during the experimental process is the load cycling, which is also demonstrated in Fig. 3. Load cycling can produce an "ed-dying-in" effect, causing the real area of contact to increase and, thereby, increasing the contact conductance. It is apparent from Fig. 3 that, in a descending contact pressure process, the thermal contact conductance is always larger than that in an ascending contact pressure process. The initial loading produced a plastic deformation of the surface contacts. Thus, when the contact pressure is decreased, the thermal contact conductance is higher than the previous value at the same contact pressure. As expected, the results for the four pairs are different due to the minor variations in the surface characteristics of the contacting surfaces, listed in Table 1. Smoother coating surfaces with lower average roughnesses had higher thermal contact conductance. Therefore, the values of uncoated joint thermal contact conductance of polished specimens are larger than turned specimens. Also, smooth-blasted specimens have larger thermal contact conductance than rough-blasted specimens.

Figures 4a–4d show magnified photographs of the aluminum specimens before and after applied contact pressure: 4a shows the polished surface magnified $800\times$ before applying the contact load, 4b shows the polished surface magnified $800\times$ after applying the contact load, 4c is the blasted-rough surface magnified $200\times$ before applying the contact load, and 4d is the blasted-rough surface magnified $200\times$ after applying the contact load. These figures illustrated the surface characteristics resulting from different surface treatments. Clearly, the surface roughness in Fig. 4b is much less than in Fig. 4a, due to the cycling contact pressure applied to the surface. In Figs. 4c and 4d, a random distribution of concave spots was observed and it is hard to distinguish the surface characteristics before and after applied pressure by observations due to the light contact pressures applied on a very rough surface. Figures 4a and 4b are polished surfaces that have fewer concave spots than blasted surfaces shown in Figs. 4c and 4d. When two blasted surfaces are brought together, the area of contact spots is much larger than that for polished surfaces. Thus, the thermal contact conductance of blasted surfaces is higher than that of polished surfaces by a factor 1.3–2.5, depending upon the contact pressure and surface topography.

The aluminum 6061-T651 specimens coated with four different materials, pure copper, copper-carbon, pure silver, and silver-carbon, were put in contact with uncoated specimens and thermally tested in a vacuum. Figure 5 illustrated the results of the experimental investigation for both pure copper and copper-carbon coatings. As can be seen with all of the

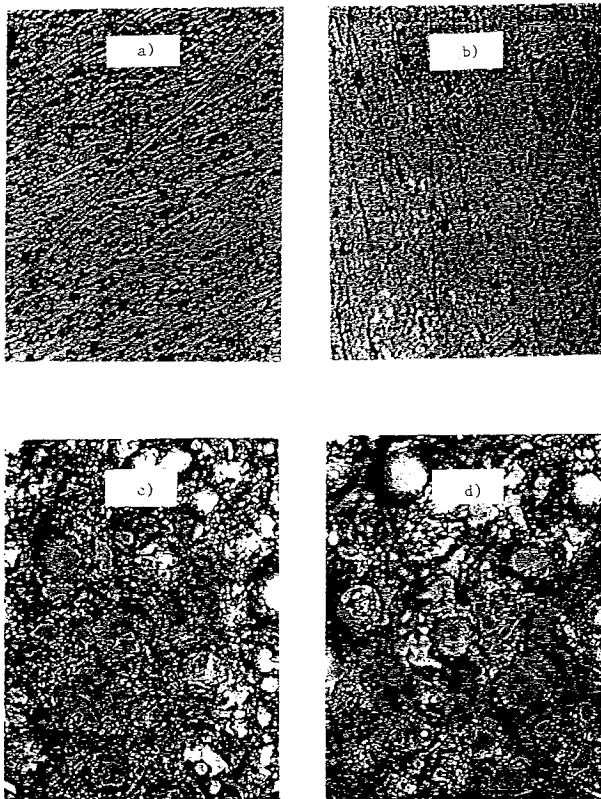


Fig. 4 Photographs of the aluminum surface before and after loading, $Ra = 0.18 \mu\text{m}$ for a) and b) and $7.92 \mu\text{m}$ for c) and d).

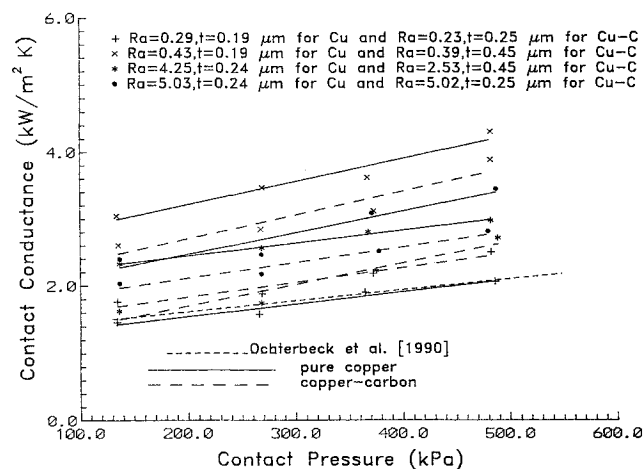


Fig. 5 Thermal test results for pure copper and copper-carbon specimens.

curves, there is an increase in the contact conductance with increase in the contact pressure. Excluding the polished surface samples the pure copper coatings improved the contact conductance over the copper-carbon phase mixture coatings by 10–20%, depending upon the surface roughness and applied contact pressure. This can be attributed to the low thermal conductivity and high microhardness of carbon. Although the polished surface did not show the same trend as the other specimens, the values of contact conductance of pure copper and copper-carbon phase mixture coatings are very close. This slight deviation is believed to be caused by some significant scratches of the coated surface of the pure copper samples. This data is also compared with data from Ochterbeck et al.,¹⁴ who reported enhancement using 51- μm -thickness copper foil. The surface roughness of the tested pair of aluminum was similar to the turned surface specimen used in this investigation, with a value of near $0.4 \mu\text{m}$. It is important to note

that the thickness of the copper foil is two orders of magnitude larger than that of the pure copper coatings.

The most significant improvements in thermal contact conductance occurred with turned surface coating specimens. It is believed that the results of the surface roughness and the coating thickness are of the same order of magnitude as for the turned surface specimen. Smooth-blasted and rough-blasted specimens produced similar results of increasing the contact conductance. However, the rough-blasted coating surface produced higher contact conductance than the smooth-blasted coating surface by a maximum of 20 and 14% for the copper-carbon and pure copper coatings, respectively. When the coating thickness was much larger than the surface roughness, the thermal contact conductance always decreased with increasing coating thickness, as in the case of polished surface specimens. The experimental results indicated that it did not significantly enhance the thermal contact conductance. An opposite effect can be obtained when the surface roughness is much larger than the coating thickness.

The pertinent test results of the pure silver and phase mixture silver-carbon coatings are shown in Fig. 6. The experimental data follow the same trend observed in the previous test, that the contact conductance increases with increasing contact pressure. Also, the thermal contact conductance of pure silver coatings are varying from 1.1 to 2.6 times higher than those of phase mixture silver-carbon coatings. Close examination of Fig. 6 reveals that the experimental data apparently consisted of two different groups: 1) one consists of polished and turned surface specimens and 2) the other consists of blasted surface specimens. It is believed that different surface characteristics are the major reason for causing two different data groups. Thermal contact conductance of blasted surface specimens is higher than that of the polished and turned surface specimens in both pure silver and phase mixture silver-carbon cases. Because the surface roughness and coating thickness are not identical in all copper and silver test specimens, the sequence of the contact conductance, from high to low, of the copper specimens is not the same as for the silver specimens with the same surface textures. In summary, the pure silver coatings obtained a contact conductance higher than the pure copper coatings by an average of 49%, and higher than the phase mixture copper-carbon coatings by an average of 68%. Furthermore, the silver-carbon coatings have an average contact conductance 1.8% less than pure copper coatings, but they have an average contact conductance 7.5% higher for phase mixture copper-carbon coatings. The high thermal conductivity value of silver might be the most important parameter for enhancing the thermal contact conductance. In Fig. 7, correlations based on an evaluation of the experimental data, including phase mixture copper-carbon and silver-carbon coating layer were proposed. Simple

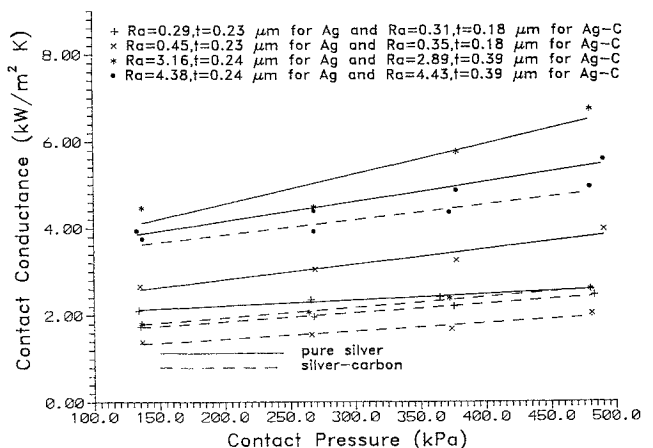


Fig. 6 Thermal test results for pure silver and silver-carbon specimens.

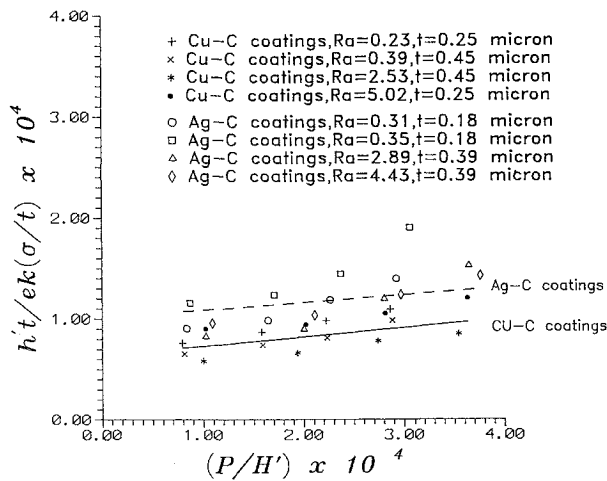


Fig. 7 Dimensionless contact conductance with the proposed correlation for copper-carbon and silver-carbon specimens.

correlations have been deduced to predict the dependence of dimensionless thermal contact conductance on the surface roughness, surface asperity slope, microhardness, contact pressure and the thermal conductivity of aluminum substrate. In addition to the individual expression for the pressure-dependent thermal contact conductance as a function of pressure, a dimensionless correlation that relates dimensionless contact conductance to the dimensionless contact pressure was developed. All the experimental data obtained were first converted to consistent SI units and then nondimensionalized. All data points for copper-carbon and silver-carbon coating layers are shown plotted on a log-log basis. As illustrated in Fig. 7, a linear regression analysis of the data revealed the following relationship between the variables for copper-carbon coatings:

$$(h't/ek')(\sigma/t)^{0.967} = 1.5 \times 10^{-4} (P/H')^{0.033} \quad (4)$$

with a rms percent difference of 18.2%. The dimensionless contact conductance results of phase mixture silver-carbon coatings are also illustrated in Fig. 7, and the correlation can be expressed as

$$(h't/ek')(\sigma/t)^{0.798} = 4.8 \times 10^{-4} (P/H')^{0.202} \quad (5)$$

with a rms difference of 15.4%.

As shown in Fig. 7 these dimensionless correlations predict the thermal contact conductance for the four surface roughnesses over a dimensionless contact range with a reasonable degree of accuracy.

To better understand the relative significance of the improvement in the thermal contact conductance, the thermal contact conductance ratio of pure material coatings are compared with phase mixture coatings. Figures 8 and 9 compare all the test data for thermal contact conductance ratio, defined as the thermal contact conductance of the coated interface with that of the uncoated interface. As shown in Fig. 8, the turned surface specimen had the highest thermal enhancement over the pressure range tested in both pure copper and phase mixture specimens. The pure copper coating obtained higher enhancement than the copper-carbon phase mixture coating in most cases, except for polished surface samples. The reason could be that the pure copper coatings have flaws such as scratches that might damage the coating surface and increase the thermal contact resistance. The same phenomenon was observed in Fig. 8, the turned surface specimens had the highest thermal enhancement for pure silver coating specimens. However, the blasted-rough specimens produced higher dimensionless contact conductance than turned surface specimens for phase mixture silver-carbon coatings. As ex-

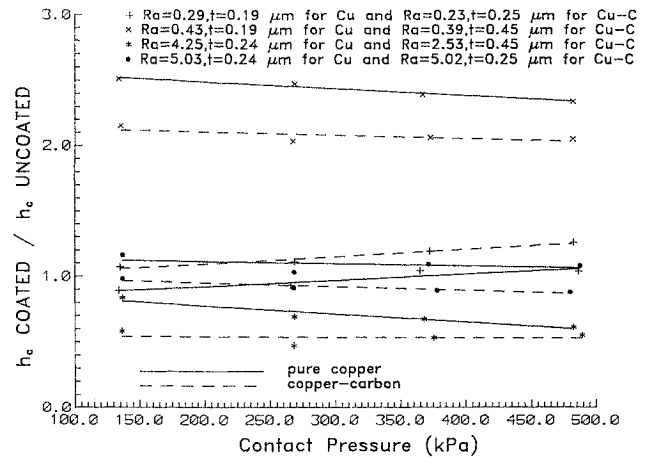


Fig. 8 Thermal contact conductance ratio for pure copper and copper-carbon specimens.

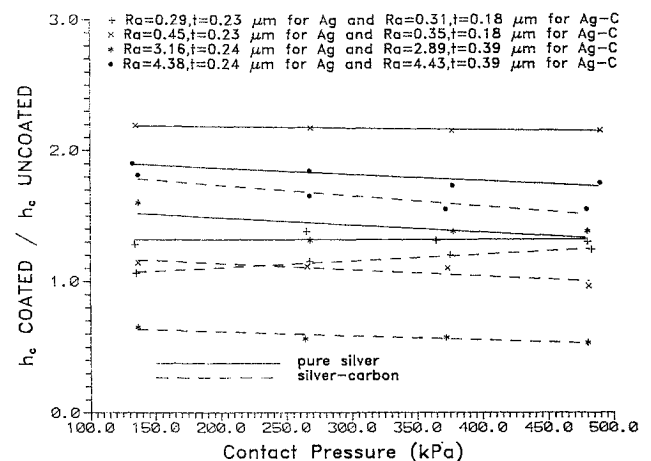


Fig. 9 Thermal contact conductance ratio for pure silver and silver-carbon specimens.

pected, the pure silver coatings produced higher thermal enhancement than phase mixture silver-carbon coatings in all cases. Although the thermal contact conductance of a pure coating layer is higher than that of a phase mixture coating layer, the adhesion strength reported by Chung et al.¹⁵ can obtain 20–240% improvement in the thermal contact conductance at the interface by phase mixture coatings. A general trend can be observed that all the coated test specimens decrease the thermal contact conductance ratio with increasing contact pressure. It is particularly true of the low contact pressure range results where variability is often encountered. Thus, from the experimental data, no definite conclusion regarding how effective different surface characteristics might affect the contact conductance can be made for a phase mixture coating under light contact pressure.

Conclusions

The use of metallic coatings to enhance thermal contact conductance has been studied experimentally. In this investigation, both primary surfaces of each pair of specimens were coated with a pure copper/silver or a phase mixture of copper-carbon/silver-carbon layer. The load cycling effect was examined and, as expected, the thermal contact conductance can be increased by cycling the load. Correlations have also been presented to predict the dimensionless thermal contact conductance of phase mixture copper-carbon and silver-carbon coating layers. Enhancement of thermal contact conductance proved greater with turned surface specimens. This is because the surface roughness and coating thickness were the same order of magnitude. The thermal contact conduc-

tance of blasted specimens was not enhanced as might have been expected, since the surface roughnesses were much larger than the coating thicknesses. The improvement of the thermal contact conductance for pure copper coatings was greater than copper-carbon phase mixture coatings by a factor of 1.1–1.3, and for pure silver coatings was greater than silver-carbon phase mixture coatings by a factor of 1.1–2.6. Although the thermal performance of pure material coatings is better than phase mixture coatings, the pure material coating layer may sacrifice robustness for thermal performance, or vice versa, depending on their required duty and life cycle. The phase mixture coating layer may indeed provide an excellent choice for some specific long-life requirements under conditions of repeated loads.

References

- ¹Thomas, T. R., and Probert, S. D., "Thermal Resistances of Some Multilayer Contacts Under Static Loads," *International Journal of Heat and Mass Transfer*, Vol. 9, 1966, pp. 739–754.
- ²O'Callaghan, W., Snaith, B., Probert, S. D., and Al-Astrabadi, F. R., "Prediction of Optimal Interfacial Filler Thickness for Minimum Thermal Contact Resistance," *AIAA Journal*, Vol. 21, No. 90, 1983, pp. 1325–1330.
- ³Chu, R. C., "Heat Transfer in Electronic Systems," *Proceedings of the 8th International Heat Transfer Conference* (San Francisco, CA), Hemisphere, 1986, pp. 293–305.
- ⁴Kraus, A. D., and Bar-Cohen, A., *Thermal Analysis and Control of Electronic Equipment*, Hemisphere, New York, 1983.
- ⁵Peterson, G. P., and Fletcher, L. S., "Thermal Contact Resistance of Silicon Chip Bonding Materials," *Proceedings of the International Symposium on Cooling Technology for Electronic Equipment*, Pacific Inst. for Thermal Engineering, Honolulu, HI, 1987, p. 438–448.
- ⁶Eid, J. C., and Antonetti, V. W., "Small Scale Thermal Contact Resistance of Aluminum Against Silicon," *Proceedings of the 8th International Heat Transfer Conference* (San Francisco, CA), 1986, pp. 659–664.
- ⁷Yovanovich, M. M., "New Contact and Gap Conductance Correlations for Conforming Rough Surfaces," *AIAA Paper 81-1164*, June 1981.
- ⁸Fletcher, L. S., "A Review of Thermal Enhancement Techniques for Electronic Systems," *IEEE Transactions of Components, Hybrids, and Manufacturing Technology*, Vol. 13, No. 4, 1990, pp. 1012–1021.
- ⁹Antonetti, V. W., and Yovanovich, M. M., "Enhancement of Thermal Contact Conductance by Metallic Coatings: Theory and Experiment," *Journal of Heat Transfer*, Vol. 107, Aug. 1985, pp. 513–519.
- ¹⁰Chung, K. C., Sheffield, J. W., and Sauer, H. J., Jr., "Effects of Metallic Coated Surfaces on Thermal Contact Conductance: An Experimental Study," 6th Miami International Symposium on Heat and Mass Transfer, Miami Beach, FL, 1990.
- ¹¹Fletcher, L. S., Blanchard, D. G., and Kinnear, K. P., "Thermal Conductance of Multilayered Metallic Sheets," *Journal of Thermophysics and Heat Transfer*, Vol. 7, No. 1, 1993, pp. 120–126.
- ¹²Kang, T. K., Peterson, G. P., and Fletcher, L. S., "Enhancing the Thermal Contact Conductance Through the Use of Thin Metallic Coating," *American Society of Mechanical Engineers Paper 89-HT-23*, Aug. 1989.
- ¹³Cassidy, J. F., and Mark, H., "Thermal Contact Resistance Measurements at Ambient Pressures of One Atmosphere to 3×10^{-12} mmHg and Comparison with Theoretical Predictions," edited by J. T. Bevens, *Progress in Aeronautics and Astronautic Thermophysics: Applications to Thermal Design of Spacecraft*, Vol. 12, 1970, pp. 23–37.
- ¹⁴Ochterbeck, J. M., Fletcher, L. S., and Peterson, G. P., "Evaluation of Thermal Enhancement Films for Electronic Packages," *9th International Heat Transfer Conference*, Hemisphere, New York, 1990, pp. 445–450.
- ¹⁵Chung, K. C., Sheffield, J. W., Sauer, H. J., Jr., O'Keefe, T. J., and Williams, A., "Thermal Contact Conductance of a Phase-Mixed Coating Layer by Transitional Buffering Interface," *Journal of Thermophysics and Heat Transfer*, Vol. 7, No. 2, 1993, pp. 326–333.

Modern Engineering for Design of Liquid-Propellant Rocket Engines

Dieter K. Huzel and David H. Huang

From the component design, to the subsystem design, to the engine systems design, engine development and flight-vehicle application, this "how-to" text bridges the gap between basic physical and design principles and actual rocket-engine design as it's done in industry. A "must-read" for advanced students and engineers active in all phases of engine systems design, development, and application, in industry and government agencies.

Chapters: Introduction to Liquid-Propellant Rocket Engines, Engine Requirements and Preliminary Design Analyses, Introduction to Sample Calculations, Design of Thrust Chambers and Other Combustion Devices, Design of Gas-Pressurized Propellant Feed Systems, Design of Turbopump Propellant Feed

Systems, Design of Rocket-Engine Control and Condition-Monitoring Systems, Design of Propellant Tanks, Design of Interconnecting Components and Mounts, Engine Systems Design Integration, Design of Liquid-Propellant Space Engines PLUS: Weight Considerations, Reliability Considerations, Rocket Engine Materials Appendices, 420 illustrations, 54 tables, list of acronyms and detailed subject index.

AIAA Progress in Astronautics and Aeronautics Series

1992, 431 pp, illus ISBN 1-56347-013-6

AIAA Members \$89.95 Nonmembers \$109.95 Order #: V-147(830)

Place your order today! Call 1-800/682-AIAA



American Institute of Aeronautics and Astronautics

Publications Customer Service, 9 Jay Gould Ct., P.O. Box 753, Waldorf, MD 20604
FAX 301/843-0159 Phone 1-800/682-2422 8 a.m. - 5 p.m. Eastern

Sales Tax: CA residents, 8.25%; DC, 6%. For shipping and handling add \$4.75 for 1-4 books (call for rates for higher quantities). Orders under \$100.00 must be prepaid. Foreign orders must be prepaid and include a \$20.00 postal surcharge. Please allow 4 weeks for delivery. Prices are subject to change without notice. Returns will be accepted within 30 days. Non-U.S. residents are responsible for payment of any taxes required by their government.